Human Molecular Genetics, 2008, Vol. 17, No. 18 **2803–2818**
doi:10.1093/hmg/ddn179
Advance Access published on June 18, 2008

Haploinsufficiency of the germ cell-specific nuclear RNA binding protein hnRNP G-T prevents functional spermatogenesis in the mouse

Ingrid Ehrmann[1], Caroline Dalgliesh[1], Aikaterini Tsaousi[1], Maria Paola Paronetto[2,3], Bettina Heinrich[6], Ralf Kist[1], Paul Cairns[1], Weiping Li[1], Christian Mueller[1,8], Michael Jackson[1], Heiko Peters[1], Karim Nayernia[1,8], Philippa Saunders[4], Michael Mitchell[5], Stefan Stamm[7], Claudio Sette[2,3] and David J. Elliott[1,*]

[1]Institute of Human Genetics, Newcastle University, Central Parkway, Newcastle NE1 3BZ, UK, [2]Department of Public Health and Cell Biology, Section of Anatomy, University of Rome 'Tor Vergata', Rome, Italy, [3]IRCSS Fondazione Santa Lucia, Rome, Italy, [4]MRC Reproductive Sciences Unit, Centre for Reproductive Biology, 49 Little France Crescent, Edinburgh EH16 4SB, Scotland, UK, [5]Génétique moléculaire de la spermatogenèse, Inserm U491, Faculté de médecine, 27, bd Jean Moulin 13385, Marseille, France, [6]Institut fur Biochemie, Emil-Fischer-Zentrum, Friedrich-Alexander Universitat Erlangen-Nurnberg, Fahrstrasse 17 91054, Erlangen, Germany, [7]Department of Molecular and Cellular Biochemistry, College of Medicine, University of Kentucky, 741 South Limestone, Lexington, KY 40536-0509, USA and [8]North East Stem Cell Institute (NESCI), Newcastle, UK

Received May 1, 2008; Revised May 29, 2008; Accepted June 16, 2008

Human *HNRNPGT*, encoding the protein hnRNP G-T, is one of several autosomal retrogenes derived from *RBMX*. It has been suggested that *HNRNPGT* functionally replaces the sex-linked *RBMX* and *RBMY* genes during male meiosis. We show here that during normal mouse germ cell development, hnRNP G-T protein is strongly expressed during and after meiosis when proteins expressed from *Rbmx* or *Rbmx*-like genes are absent. Amongst these *Rbmx*-like genes, DNA sequence analyses indicate that two other mouse autosomal *Rbmx*-derived retrogenes have evolved recently in rodents and one already shows signs of degenerating into a non-expressed pseudogene. In contrast, orthologues of *Hnrnpgt* are present in all four major groups of placental mammals. The sequence of *Hnrnpgt* is under considerable positive selection suggesting it performs an important germ cell function in eutherians. To test this, we inactivated *Hnrnpgt* in ES cells and studied its function during spermatogenesis in chimaeric mice. Although germ cells heterozygous for this targeted allele could produce sperm, they did not contribute to the next generation. Chimaeric mice with a high level of mutant germ cells were infertile with low sperm counts and a high frequency of degenerate seminiferous tubules and abnormal sperm. Chimaeras made from a 1:1 mix of targeted and wild-type ES cell clones transmitted wild-type germ cells only. Our data show that haploinsufficiency of *Hnrnpgt* results in abnormal sperm production in the mouse. Genetic defects resulting in reduced levels of *HNRNPGT* could, therefore, be a cause of male infertility in humans.

INTRODUCTION

The heterogeneous ribonucleoproteins (abbreviated hnRNPs) are a family of nuclear RNA binding proteins with roles in nuclear RNA metabolism including the regulation of pre-mRNA splicing (1). HnRNP G-T (an acronym of **h**eterogen**e**ous **r**ibo**n**ucleo**p**rotein **G** expressed in the **T**estis) is a testis-specific hnRNP encoded by an autosomal retrogene

*To whom correspondence should be addressed. Tel: +1 912418694; Fax: +1 912418666; Email: david.elliott@ncl.ac.uk

(*HNRNPGT*) on human chromosome 11p15. Sequence homology suggests that the *HNRNPGT* gene is derived from retrotransposition of a transcript from the X-linked *RBMX* gene (which encodes the nuclear hnRNPG protein) (2). X-linked retrogenes are thought to be important during pachytene of male meiosis when the sex chromosomes of mammals are inactivated by a process called Meiotic Sex Chromosome Inactivation and relocate in a nuclear structure called the XY body (3–5). The XY body is repressive for transcription, but a number of autosomal retrogenes derived from X-linked genes are meiotically expressed. These autosomal retrogenes may encode either direct functional replacements for essential X-linked housekeeping genes such as *PGK1* which are turned off during meiosis, more specialized germ cell proteins with distinct functions from their X-linked counterparts, or possibly play a post-meiotic role to normalize gene expression between X- and Y-chromosome containing round spermatids (6).

Consistent with a role in meiosis, human hnRNP G-T protein is highly expressed in the nuclei of primary spermatocytes and in round spermatids (2). However in addition to *HNRNPGT*, there are 9 other retrogene copies of RBMX in the human genome, including a full length copy on chromosome 1 which is more closely similar to *RBMX* (*RBMXL1*) than *HNRNPGT*, and a slightly truncated version on chromosome 9 (*RBMXL9*) (7). Expression analysis of these genes using RT–PCR has shown that *RBMXL1* is expressed ubiquitously (including within the testis) while *RBMXL9* expression is restricted to brain and testis. The presence of two other full-length and more closely related *RBMX* retrogenes in the human genome (7) and at least one in the mouse (8) suggest the hypothesis that these other retrogenes might in fact replace *RBMX* gene function during meiosis, and that *Hnrnpgt* might have evolved distinct functions.

Because of its testis-specific expression, defects in the *HNRNPGT* gene might play a role in human infertility. Sequence variations in the *HNRNPGT* gene have been identified in men with impaired fertility, and hnRNPGT protein is not expressed in men showing incomplete spermatogenesis (9,10). *HNRNPGT* is also implicated with a role in infertility through its sequence homology to the Y-linked *RBMY* genes (2). *RBMY* genes were originally identified by positional cloning as candidates for a Y chromosome gene deleted in some infertile men called the *Azoospermia factor* (*AZF*) and microdeletions of the *AZFb* region of the human Y chromosome prevent expression of RBMY protein (11,12). Deletions which reduce mouse *Rbmy* gene copy number are also associated with sperm abnormalities (13) and *Rbmy* genes are conserved in all mammals suggesting a fundamental role in male germ cell development which was established early in mammalian evolution (14). However, because mouse *Rbmy* is a multiple copy gene on the Y chromosome, it is technically difficult to inactivate by gene targeting in mice.

Here we have analysed the genetic history and expression patterns of *Hnrnpgt* compared with *Rbmx* and other *Rbmx*-derived retrogenes, and tested the function of *Hnrnpgt* in mouse germ cell development by gene targeting in mice. Our results point to a unique and important function for hnRNP G-T protein in meiotic and post-meiotic germ cell development.

RESULTS

HNRNPGT orthologues are present in all superorders of placental mammals and are under positive selection

An antiserum raised against human hnRNP G-T protein identified a testis-specific protein in mouse and bull suggesting the existence of an hnRNP G-T orthologue in these species (2). If the *HNRNPGT* gene indeed performs a basic biological function during germ cell development, this function would be expected to be conserved between species. To test this, we searched for genes in other species which are both retrogenes (i.e. do not contain introns) and map to genomic regions syntenic to the human *HNRNPGT* gene (adjacent to the *NLRP14* gene within the genomic sequence). Using these criteria, we found putative *HNRNPGT* orthologues in species representing three of the four super-orders of placental mammals (15); Laurasiatheria (mouse and rat), Euarchontoglires (macaque and shrew) and Afrotheria (elephant and tenrec). A retrogene was also identified in one Xenarthran species (armadillo), although because of the incomplete genome sequence a syntenic relationship with the human *HNRNPGT* gene could not be confirmed. This species distribution is consistent with *HNRNPGT* being created by a single retrotransposition event before the radiation of placental mammals. Using the same criteria, we were unable to identify *HNRNPGT* orthologues in any marsupial genome.

To investigate the relationship between putative *HNRNPGT* orthologues and *RMBX* further we used the sequences identified, together with *RBMX* sequences from the same species (where available) to construct phylogenetic trees with the *RBMX* orthologue from chicken serving as an outgroup (Fig. 1). In this tree, the *HNRNPGT* and *RMBX* sequences form two distinct clades with 100 and 97% bootstrap support, respectively. In both clades, some branching orders are inconsistent with known phylogenetic relationships (15), most noticeably the positioning of the tenrec and cow *HNRNPGT* genes. The position of these genes within the tree does not have high bootstrap support, highlighting the uncertainty of the inferred relationships. What is clear is that the basic topology of the tree is consistent with the *HNRNPGT* sequences being created from a single retrotransposition event which occurred before the radiation of eutherian mammals. Importantly, the branch lengths within the *HNRNPGT* and *RBMX* clades are different. This could be explained by a strong selection for conservation of function acting upon *RBMX*, with *HNRNPGT* evolving faster. More rapid evolutionary change might indicate *HNRNPGT* is under less selective pressure, or might be because of the increased evolutionary rate of genes involved in reproductive processes (16). The branch lengths in the phylogenetic tree show that *HNRNPGT* is less conserved than *RBMX*. This is evident from the rate of non-synonymous substitutions (Ka) between human and mouse *RBMX* (0.006) and human and mouse *HNRNPGT* (0.109) and also reflected in the Ka/Ks ratio which is 10 times higher for HNRNPGT (0.20) than RBMX (0.02) (Supplementary Material, Tables S1a and 1b). The observed Ka/Ks ratio of less than 1 demonstrates that the coding sequence of HNRNPGT has been conserved, but indicates that, compared to RBMX, it has been subject to reduced selection pressure and/or positive selection for amino acid substitutions (see legend to Supplementary Material, Table S1).

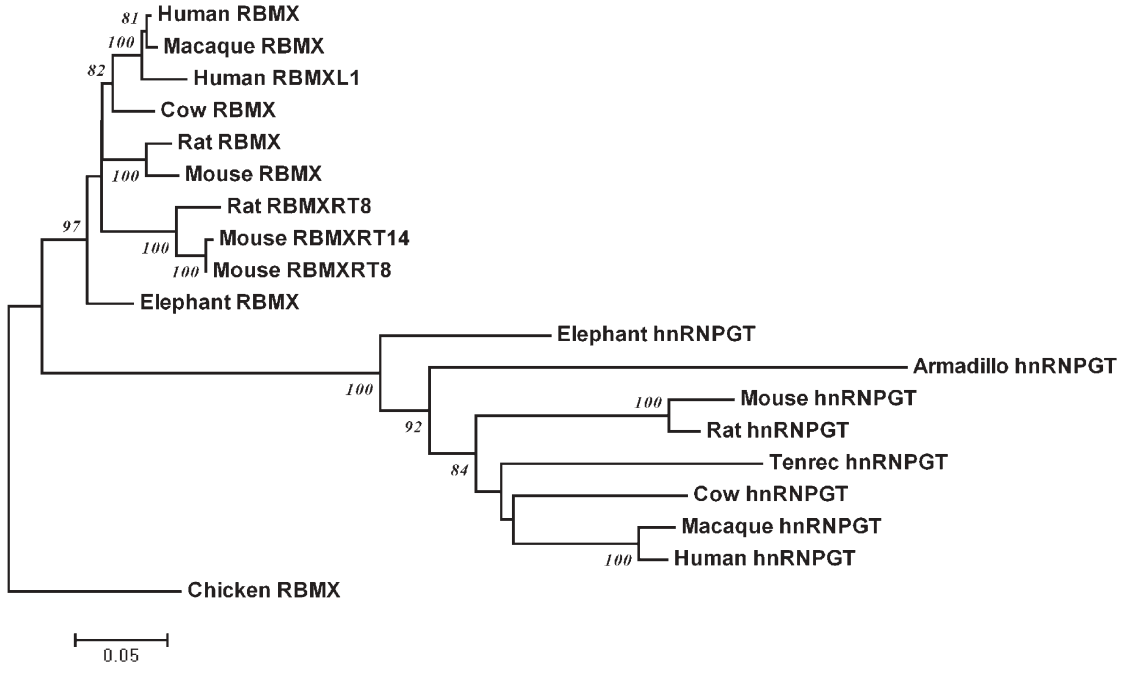

Figure 1. *HNRNPGT* originated from a single retrotransposition event before the radiation of all extant placental mammals. Neighbour joining phylogenetic tree of mammalian *RBMX* and *HNRNPGT* related sequences constructed using the maximum composite likelihood method (46). Bootstrap values over 70% are shown, based on 1000 replicates. For details, see Materials and Methods. Mouse *Rbmxrt8* and *Rbmxrt14* retrogenes also formed a clade with 100% bootstrap support, indicating that *Rbmxrt14* is a retroposed copy of the *Rbmxrt8* gene (rather than both being independently derived from *Rbmx*; see Supplementary Material, Fig. S1).

The mouse genome contains two additional *Rbmx*-derived retrogenes which have evolved in the rodent lineage but only one of them is expressed

Our gene search in the mouse genome revealed two additional full-length mouse *Rbmx*-derived retrogenes (Chromosome 14 copy, *Rbmxrt14*: ENSMUSG00000049235; Chromosome 8 copy, *Rbmxrt8*: ENSMUSG00000037070) which could potentially encode proteins which are greater than 95% identical to RBMX (Fig. 2: by comparison *Hnrnpgt* encodes a protein which is only around 75% identical to *Rbmx*). Neither *Rbmxrt8* nor *Rbmxrt14* are conserved in human, but an orthologue of *Rbmxrt8* is found on rat chromosome 19 (Ensembl gene identification number ENSRNOG00000012138). This means that *Rbmxrt8* and *Rbmxrt14* evolved in the rodent lineage respectively before and after the mouse/rat divergence. Comparative analysis shows that *Rbmxrt14* is a retroposed pseudogene (legend to Fig. 1) derived from a spliced *Rbmxrt8* transcript bearing the shorter form of the 5′-UTR (see legend to Supplementary Material, Fig. S1). *Rbmxrt8* is under greater selective constraint than *Rbmxrt14* (Supplementary Material, Table S2a and b) and there are many *Rbmxrt8* ESTs in the databases from a range of tissues, although we were unable to find a single EST derived from *Rbmxrt14*. Taken together, these data suggest that *Rbmxrt8* is expressed and *Rbmxrt14* is not.

Mouse hnRNP G-T is exclusively expressed after the initiation of meiosis

The above analysis identified an *HNRNPGT* gene (ENSMUSG00000073894, also known as *Rbmxl2*) located on a region of mouse chromosome 7 which is syntenic to human chromosome 11p15 where human *HNRNPGT* is located. Consistent with ENSMUSG00000073894 being the mouse orthologue of human *HNRNPGT*, Northern blotting identified a single transcript of ~1500 nucleotides from ENSMUSG00000073894 exclusively in mouse testis (Fig. 3 and data not shown). In addition, we raised specific antisera to mouse hnRNP G-T and demonstrated by western blotting that the protein is also testis-specific (Supplementary Material, Fig. S2). Northern blotting of RNA isolated from different mouse tissues detected expression of *Rbmx*, *Rbmxrt8* and *Hnrnpgt* within the testis, along with expression of the testis-specific *Rbmy* gene. While *Hnrnpgt* expression was testis-specific, co-expression of the *Rbmx* and *Rbmxrt8* genes was particularly evident in thymus, spleen, testis and brain which are tissues containing extensive alternative mRNA splicing programmes (Fig. 3). Two splice variants of the *Rbmx* transcript with alternative 3′ ends (8) were also differentially expressed between tissues. Of these *Rbmx* alternative transcripts, splice variant 2 was highly expressed in the testis but splice variant 1 was not detectably expressed, although it has been detected by RT–PCR and was originally isolated from a testis cDNA library (8).

Since the Rbmxrt8 protein sequence is more similar to RBMX than the hnRNP G-T protein sequence and the *Rbmx*, *Rbmxrt* and *Hnrnpgt* genes are co-expressed within the testis (Figs 2 and 3), we considered the possibility that RBMXRT8 protein might in fact provide a more similar replacement for RBMX protein function during meiosis. To test if the cognate proteins from these genes were co-expressed in the same cells during germ cell development, we carried out

A

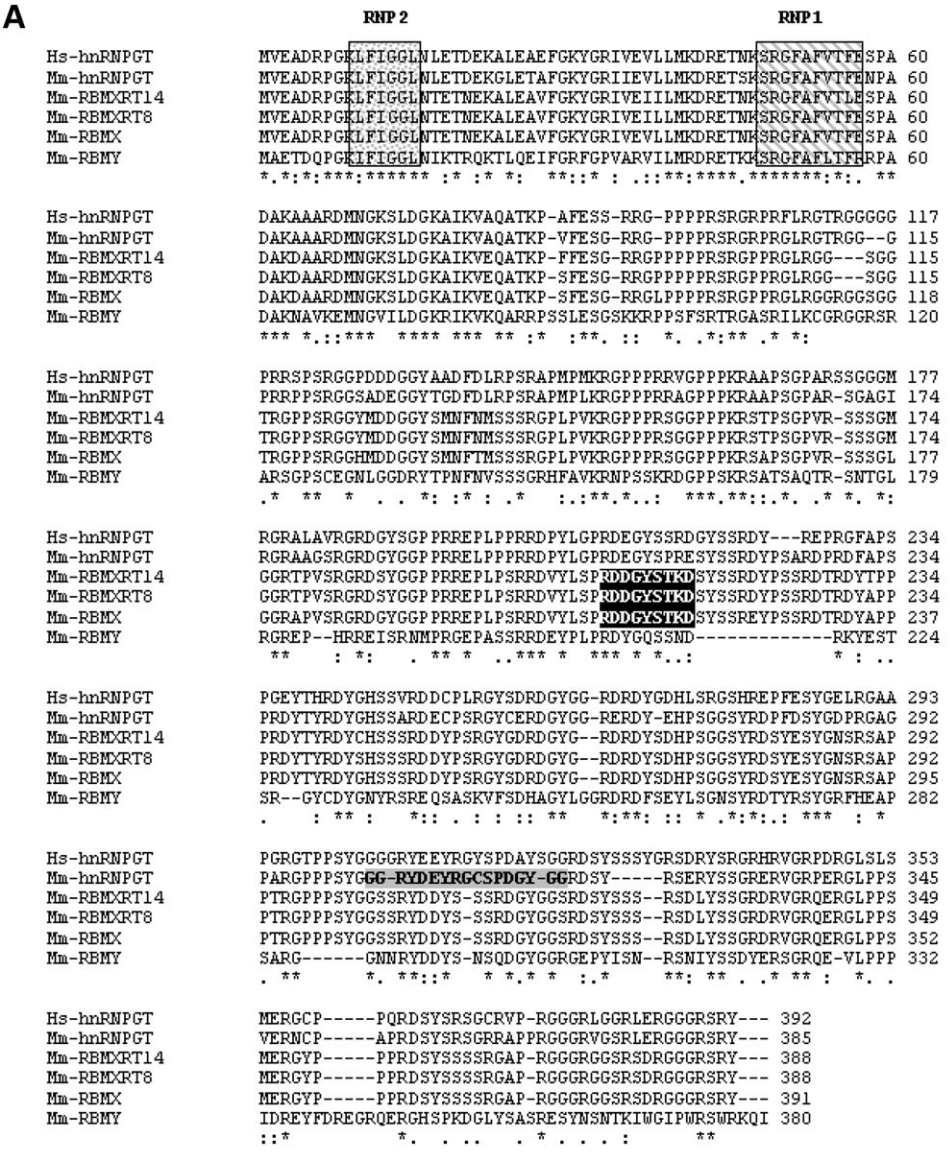

B

	Hs RBMX	Hs hnRNPGT	Mm hnRNPGT	Mm RBMX	Mm RBMXL8	Mm RBMXL14	RBMY
Mm hnRNPGT		79.3% I 85.1% S	-	75.1%I 83.2%S	74% I 82.4% S	73.2%I 81.9%S	41.6% I 49.2% S
Mm RBMX	98.7% I 99.2% S			-	96.4% I 97.4% S	95.4% I 96.7% S	44.9% I 58.2% S

Figure 2. A family of RBMX proteins are encoded by the mouse genome. (**A**) The protein sequence of human (Hs) hnRNPG-T protein aligned with the conceptual protein sequences encoded by the open reading frames of mouse (abbreviated Mm) *Hnrnpgt* (encoded by chromosome 7), *Rbmx* (hnRNPG, encoded by the X chromosome), *Rbmxrt8* (encoded by chromosome 8) and *Rbmxrt*14 (encoded by chromosome 14). Conserved sequences within the N terminal RNA recognition motif which is found within each of these proteins are boxed and striped (RNP1), or stippled (RNP2). The 18 amino acid peptide which was used to generate and affinity purify the α-mouse HnRNP G-T specific polyclonal antibody is lightly shaded, and the actual peptide sequence is in bold. The peptide to which the antisera specific to RBMX, RBMXRT8 and RBMXRT14 proteins was raised is indicated by a black box. (**B**) Table showing percentage sequence identity (I) and similarity (S) between human and mouse hnRNPGT proteins, and between different members of the mouse RBM protein family measured using a pairwise alignment algorithm (http://www.ebi.ac.uk/emboss/align/index.html).

further experiments using our antisera to hnRNP G-T and RBMX. To differentiate between cell types in the testis, we used three approaches. First, on western blots containing protein extracted from purified germ cell populations isolated by elutriation (17), no hnRNP G-T protein expression was detected in spermatogonia but strong hnRNP G-T protein expression was detected in primary and secondary spermatocytes, and somewhat weaker expression in round spermatids

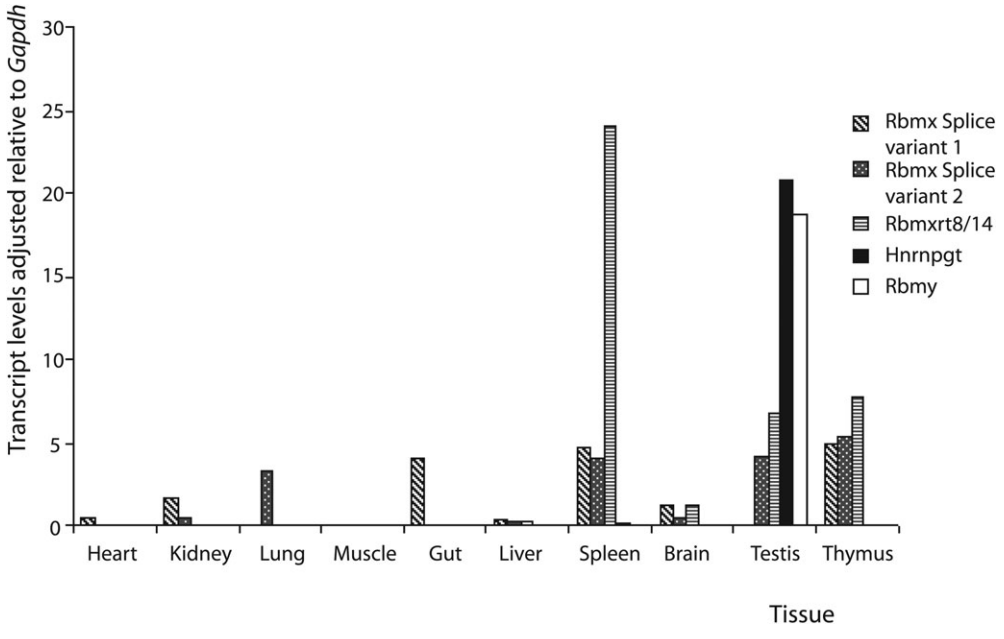

Figure 3. The *Hnrnpgt*, *Rbmx* and *Rbmxrt8* genes are co-expressed in the testis. Bar chart showing expression of mouse *Rbmy*, *Rbmx* splice variants 1 and 2, *Hnrnpgt*, and *Rbmxrt8* genes quantitated by northern blotting and normalized to the expression of *Gapdh* in different mouse tissues.

(Fig. 4A, middle panel). In contrast, high RBMX and RBMXRT8 protein expression was detected in purified spermatogonia, but not in the later stages of spermatogenesis (Fig. 4A, upper panel). An Erk2 loading control confirmed equal levels of protein loading in each lane.

Secondly, we probed western blots containing testis protein from mice going through the first wave of germ cell development, which contain germ cells enriched in specific stages of spermatogenesis. HnRNP G-T protein expression was low until day 13 (when germ cells are initiating meiosis I), and thereafter strong (Fig. 4B, middle panel). Parallel western blots showed that RBMX/RBMXRT8 protein expression was high in the testes of 4-day-old mice (when spermatogonia represent the sole germ cells in the testis) and low later on (as spermatogonia become diluted by later stages of germ cell differentiation) (Fig. 4B, top panel).

Thirdly, we used the affinity purified α-mouse hnRNP G-T antiserum to examine the expression pattern of hnRNP G-T protein on mouse testis sections using indirect immunofluorescence. High levels of expression were detected in the nuclei of primary spermatocytes, and to a lesser extent in round spermatids (abbreviated Sp and Rtd, respectively, in Fig. 4C). There was no detectable expression in spermatogonia (abbreviated Spg: only DAPI fluorescent counterstain was visible, pseudocoloured blue in Fig. 4C). This pattern of expression identified by immunostaining was similar to that previously observed for human hnRNP G-T (2). RT–PCR experiments have reported expression of the human *RBMX*-related retrogenes *RBMXL1* and *RBMXL9* in the testis (7). The peptide used to raise the antisera against mouse RBMX protein is also encoded within the Open Reading Frames of human RBMX and the RBMXL1 and RBMXL9 retrogenes. Consistent with the mouse data above, immunohistochemistry on human testis sections showed strong expression of RBMX/RBMXL1/RBMXL9 protein only in pre-meiotic stages of human germ cell development and within the nuclei of somatic Sertoli cells (abbreviated as SC in Fig. 4D: in this section the brown corresponds to specific staining by the antibody while the blue is the haematoxylin counterstain).

These results indicate that the mouse hnRNPGT protein has a similar pattern of expression to its human orthologue (2) suggesting similar meiotic and post-meiotic functions for hnRNPGT protein in human and mouse. Hence, *Hnrnpgt* has acquired a promoter which is active during and after meiosis. In contrast, the RBMX and RBMXRT 8 proteins are only detectably expressed prior to meiosis. Because of its lack of expression in meiosis, *Rbmxrt8* would be unable to provide an alternative meiotic replacement function for *Rbmx*.

Mouse chimaeras made from TBV-2 ES cells containing a targeted disruption of the *Hnrnpgt* gene did not transmit the targeted allele

Our expression analyses indicated that hnRNP G-T is the only source of an RBMX-like protein during and after meiosis in the mouse and human testis. To test if *Hnrnpgt* gene expression is important for normal germ cell development, we inactivated one *Hnrnpgt* allele by gene targeting in TBV-2 ES cells using a construct in which the majority of the *Hnrnpgt* gene is replaced by the *lacZ* gene (Fig. 5C). A correctly targeted ES cell clone (2.1D3) was isolated and injected into blastocysts resulting in the generation of seven chimaeras (six male and one female). This distortion in the sex ratio of chimaeric pups is indicative of good quality chimaeras, as were high levels of coat chimaerism (18,19). However, over the course of 9 months of breeding, the five fertile chimaeric males and one female produced 291 black pups but no agouti pups (indicative of transmission of the

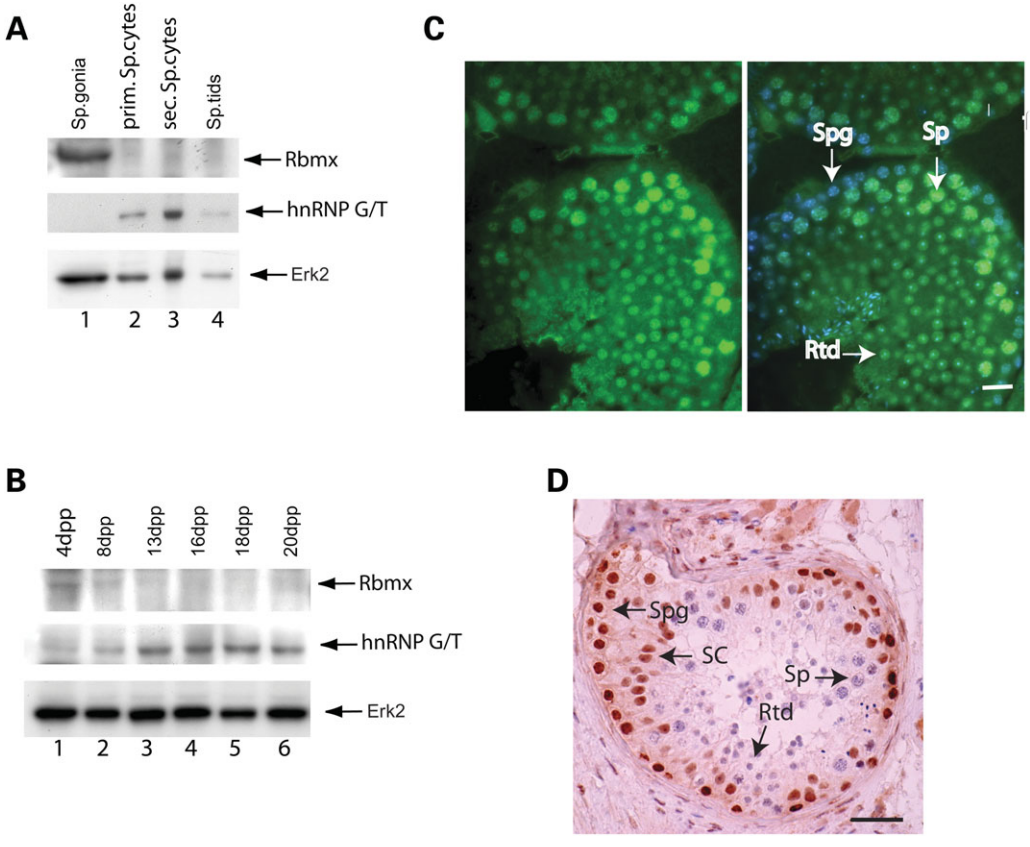

Figure 4. hnRNPGT provides exclusive RBMX family function during meiosis. (**A**) Mouse germ cells were purified by elutriation, proteins extracted and western blotted. Blots were probed with an antisera raised to a peptide sequence in RBMX/RBMXRT proteins (upper panel) or the affinity purified α-HnRNPG-T antisera (middle panel) and α-Erk2 (lower panel). We confirmed equal loading of protein in each lane using an antibody against Erk2 (lower panel). (**B**) Mouse testes from different developmental stages from 4 to 20 days postpartum were western blotted and probed with antisera as in part (A). (**C**) Mouse hnRNP G-T protein detected by the affinity purified α-HnRNPG-T antisera is highly expressed in the nuclei of primary spermatocytes. Left-hand panel: antibody staining was visualized using indirect immunofluorescence (pseudocoloured green). Right-hand panel shows the same picture including a DNA counterstain (DAPI, blue colour) which indicates that the cells on the periphery of the seminiferous tubules (Spermatogonia or Spg) are only stained for DAPI, while the meiotic spermatocytes (Sp) and post-meiotic round spermatids (Rtd) strongly express hnRNP G-T (pseudocoloured green). The scale bar represents 10 μm. (**D**) Human testis probed with an antisera raised to a peptide sequence in RBMX/RBMXRT proteins and detected using an HRP-conjugated secondary antibody. Brown staining indicates RBMX/RBMXRT protein detection, and blue staining is the haematoxylin counterstain.

ES cell genome). Full breeding data for these TBV-2 ES cell-derived chimaeras is given in Supplementary Material, Table S3.

These experiments suggested that germ cells which contained a heterozygous disruption of the *Hnrnpgt* gene were unable to contribute to the germline. This might have been because of either (i) haploinsufficiency of the *Hnrnpgt* gene or (ii) some other problem with the line of ES cells used in the experiment. A published analysis of ES cells which had successfully gone germline showed that a level of euploidy of greater than 50% is a good prognostic indicator of germline transmission (18). We found that more than 90% of the cells in clone 2.1D3 were euploid (Table 1). The TBV-2 ES cell line we used in the above targeting experiments had also recently provided germline transmission of different targeted alleles in four other cases (20,21). However, in order to eliminate the possibility that the failure to transmit the targeted allele was the result of an undetected problem with our TBV-2 cell line, we carried out a further round of gene targeting in a second ES cell line E14.1.

Fertile chimaeric mice containing a high frequency of E14.1 ES-derived germ cells with a targeted disruption in *Hnrnpgt* did not transmit the targeted allele

After re-targeting, we chose two new independently targeted ES cell clones 2.1G5 and 3.1B11 for further analysis and characterized these cell lines using Southern blot analysis to confirm precise integration by our targeting vector (Fig. 5A and B). The Southern blot also showed that clone 2.1G5 contains a homogeneous population of ES cells containing the targeted allele (Fig. 5A and B). Eighty-seven percent of cells within the 2.1G5 clone had a normal euploid karyotype (Table 1). Clone 2.1G5 was used to generate chimaeras which were again good quality according to the above criteria. Three high percentage coat colour chimaeras C1, C5 and C8 derived from the 2.1G5 cell line were fertile (Supplementary Material, Table S4). We then assessed the level of chimaerism at the DNA level using a strain-specific PCR (see methods) and detected a contribution of 10–15% of 129 genotype cells within the testes of chimaeras C1 and C8 (Fig. 6).

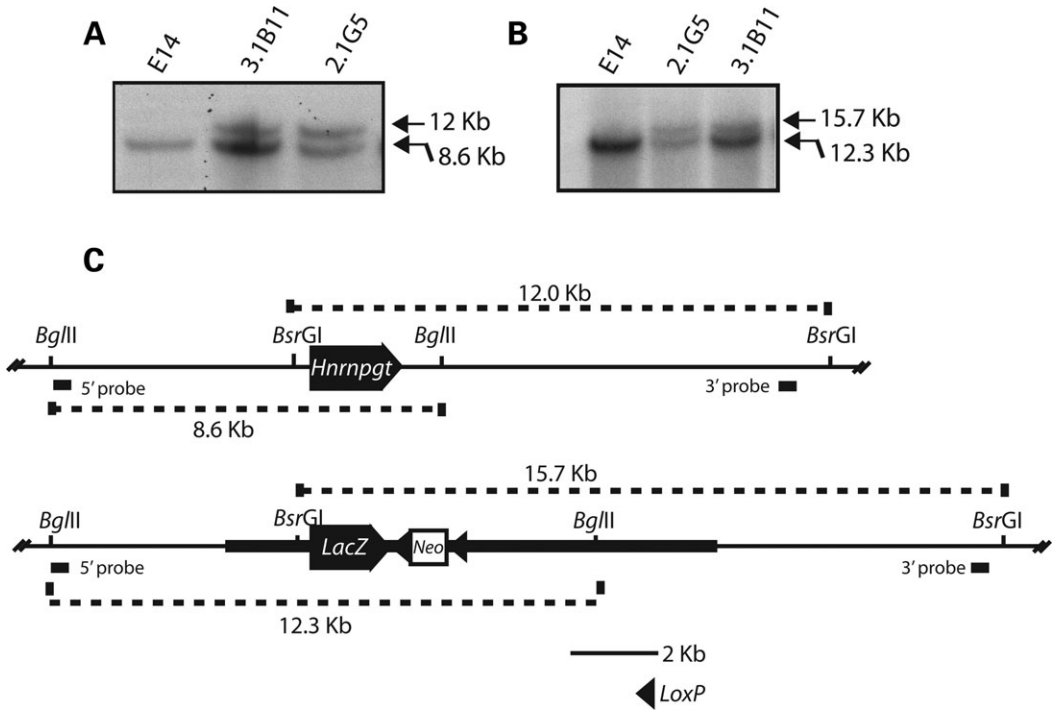

Figure 5. Targeting of the *Hnrnpgt* gene in ES cells by homologous recombination. (**A**) Southern blot of genomic DNA from E14 ES cells, and the 3.1B11 and 2.1G5 clones after digestion with *Bgl*II. The blot was probed with the 5′ probe and developed by autoradiography. (**B**) Southern blot of genomic DNA from E14 ES cells, and the 3.1B11 and 2.1G5 clones after digestion with *Bsr*GI. The blot was probed with the 3′ probe and developed by autoradiography. (**C**) Map of the wild-type *Hnrnpgt* genomic locus (above) and the targeted loci (below) showing the positions of the Hnrnpgt gene and LacZ transgene, restriction sites used in the analysis and location of the 5′ and 3′ probes. Above each restriction map are shown the fragments detected by the 3′ probe in the wild-type and targeted locus, and below the restriction map are shown the fragments detected by the 5′ probe. Southern blots of restriction digested genomic DNA from clone 3.1B11 confirmed the genomic structure of the wild-type and targeted alleles within the ES cells. However, these blotting experiments detected the restriction fragment corresponding to the wild-type allele slightly more strongly than that of the targeted allele. Since there is one targeted allele and one wild-type allele per ES cell, the theoretically expected ratio for a pure clone of heterozygote ES cells containing a targeted allele should be 50:50. Consistent with this, phosphorimager analysis confirmed that clone 2.1G5 gave a ratio of 50:50. Clone 3.1B11 gave a ratio of 70:30. This is very close to the expected ratio of 75:25 if clone 3.1B11 contained one wild-type (untargeted) ES cell for every targeted ES cell (in this case, there would be three wild-type alleles for every targeted allele). This indicated that clone 3.1B11 contains a mixture of targeted ES cells and untargeted ES cells at an approximate ratio of 1:1.

Table 1. Karyotype analysis of each of the ES cells used in this study

ES cell clone	ES cell line	Euploid karyotypes (%)
2.1D3	TBV-E2	93
2.1G5	E14	87
3.1B11	E14	70

Despite this level of chimaerism for 129-derived cells, C1 and C8 produced between them in excess of 200 Bl6 pups and only 7 agouti pups. Although the Mendelian expectation is that the transgene should be transmitted to ∼50% of the offspring, none of the pups contained the targeted allele when assayed by either genomic PCR or Southern blotting (not shown).

To establish if 129 cells containing the targeted disruption of *Hnrnpgt* were able to contribute efficiently to the germline, we carried out immunohistochemistry with a rabbit polyclonal antibody specific to the bacterial LacZ protein. Strong LacZ protein expression was detected within 10–15% of seminiferous tubules from chimaeras C1 and C8 (Fig. 6). When LacZ was expressed, it recapitulated expression detected for the endogenous hnRNP G-T protein: no LacZ staining was detected within spermatogonia; however, strong expression was detected in meiotic and post-meiotic germ cells (compare Fig. 7D with Fig. 4C). No immunohistochemical signal was detected in the testis of a wild-type C57Bl6 mouse (Fig. 7C), or when normal rabbit serum was used instead of the primary anti-LacZ antibody (not shown). Chimaera C5 was particularly informative. Although C5 contained a ∼30% ES129 contribution assayed by the strain-specific PCR (Figs 6 and 8C) or LacZ staining (Figs 6 and 7D), all 79 pups sired by this chimaera had black coat colour. To establish why the ES cell-derived sperm produced from C5 did not sire offspring, we compared the relative proportions of each genotype in genomic DNA from the testis, sperm from the epididymus of the chimaera and sperm collected from the uterus of a plugged DBA strain female. ES129-derived cells were detectable in the testes of C5 (Fig. 8C, lanes 5 and 6), at slightly reduced levels relative to C57Bl6 sperm in the epididymus (Fig. 8C, lanes 3 and 4) and then were undetectable as sperm within the uterus (Fig. 8C, lane 2: notice in this lane that the PCR product from the C57Bl6 sperm is still clearly visible). However, although we could not detect 129-derived sperm by strain-specific PCR, the targeted allele could be detected by gene-specific PCR (see Methods) in uterine sperm from chimaera C5 suggesting the presence of sperm cells containing the targeted allele at low levels (Fig. 8G, lane 7).

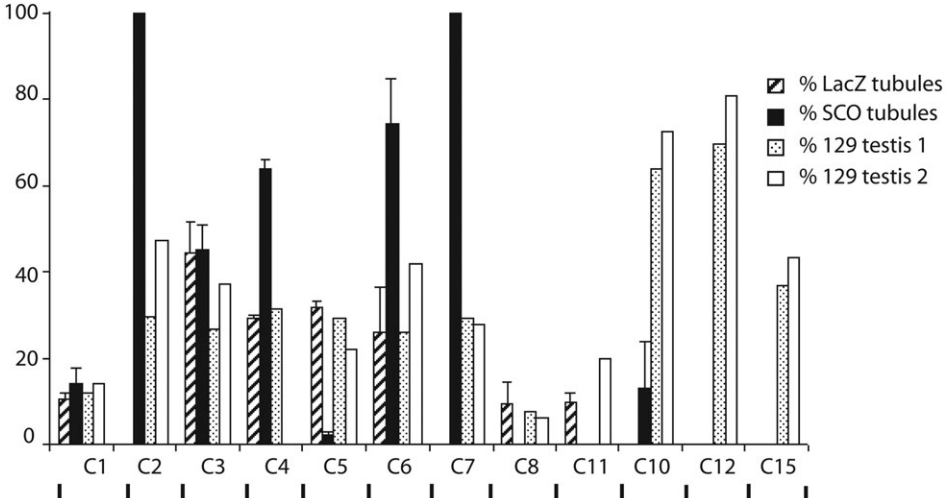

	C1	C2	C3	C4	C5	C6	C7	C8	C11	C10	C12	C15
Morphology	Mixed	SCO	Mixed	Mixed	Mixed	Mixed	SCO	Mixed	Mixed	Normal	Normal	Normal
Av. litter size	6.4	0	0	0	6.8	0	0	8	6.8	7.7	7.6	6.5
Sperm count x106	3.3 2.8	0 0	0.78 0.24	0 ND	ND ND	0 ND	0 0	8.3 12	12 12	12 12	11.3 11.5	11 9.65
Testis Wt. (grams)	0.066 0.063	0.009 0.019	0.025 0.039	ND ND	ND ND	0.0135 0.014	0.0172 0.0162	0.0625 0.066	0.094 0.112	0.071 0.083	0.097 0.096	0.102 0.107
Strain of progeny	146 Bl6 7 Ag	0	0	0	79 Bl6	0	0	51 Bl6	135 Bl6 4 Ag	0 Bl6 108 Ag	4 Bl6 146 Ag	73 Bl6 41 Ag
Cell line	2.1G5	2.1G5	2.1G5	2.1G5	2.1G5	2.1G5	2.1G5	2.1G5	3.1B11	3.1B11	3.1B11	3.1B11

Figure 6. Summary of experimental data obtained from chimaeras. For genotyping, the intensity of the bands was measured after strain-specific genomic PCR amplification and agarose gel electrophoresis and plotted as a percentage. The percentage of LacZ positive tubules and SCO tubules are the means of between two and seven separate sections from different parts of the testes.

A group of infertile high percentage chimaeric mice made from targeted E14.1 ES cells produced abnormal sperm

Another group of 2.1G5-derived chimaeric males were infertile (C3, C4 and C6) but produced sperm. Sections from the testes of these mice showed a mixed phenotype: some seminiferous tubules were sertoli cell only (SCO), but others contained a complete complement of germ cells (Fig. 7B and E). The level of testicular chimaerism detected within chimaeras C3, C4 and C6 was quite high (between 27 and 42% 129 genotype using the strain-specific genomic PCR) and in each case was comparable to that detected in the kidney (Fig. 8A and B). The majority of seminiferous tubules from chimaeras C3, C4 and C6 which contained germ cells also stained positive for LacZ protein, indicating that the germ cells contained the targeted gene disruption of *Hnrnpgt* (Fig. 7B). In some cases, residual LacZ positive germ cells were also visible in otherwise SCO tubules, suggesting these SCO tubules had originally contained germ cells expressing the lacZ gene (indicated by an arrowhead in Fig. 7E). Other tubules from C3, C4 and C6 which were devoid of germ cells also frequently contained groups of sloughed off cells which might be germ cell-derived (arrowed in Fig. 7E).

Although they were infertile, C3, C4 and C6 produced 129 ES cell-derived epididymal sperm which could be detected at a high level by strain-specific PCR compared with C57Bl6-derived sperm (Fig. 8A, lanes 6–15 and Fig. 8B lanes 2 and 3). The gene-specific PCR also detected the targeted transgene in the epididymal sperm from these chimaeras (Fig. 8G). Since they contained high levels of the targeted allele, we examined the morphology of the epididymal sperm from chimaeras C3, C4 and C6. Chimaeras C3, C4 and C6 produced sperm with high frequencies of sperm abnormalities (Fig. 9G). These sperm abnormalities included abnormal sperm heads (indicated as black arrowheads in Fig. 9A–E) and abnormal sperm tails (Fig. 9E). In chimaeras 3 and 6, both abnormal and normal sperm were seen, although in C4 virtually all the sperm were abnormal in morphology (Fig. 9A, B and G). The morphology of normal mouse sperm is shown in Figure 9F (normal sperm head morphology is indicated with a white arrow head).

Some high percentage infertile mouse chimaeras derived from targeted E14.1 ES cells were azoospermic

Two further chimaeras (C2 and C7) were also infertile, had particularly small testes (the testes of chimaera 7 next to a C57Bl6 littermate is shown in Fig. 7A) and did not produce any sperm. Sections of these testes showed they contained seminiferous tubules apparently devoid of germ cells (Fig. 7F). Both chimaeras C2 and C7 had a 30–50% ES129 cell contribution to the testis relative to C57Bl6 at the level of genomic DNA (Fig. 6, Fig. 8A, lanes 3–4 and Fig. 8B, lanes 5–6). Not even C57Bl6 sperm were produced by chimaeras C2 and C7: no sperm were detected within the epididymus and only a DBA strain genomic PCR signal was detected in a uterine sample of female DBA mice plugged

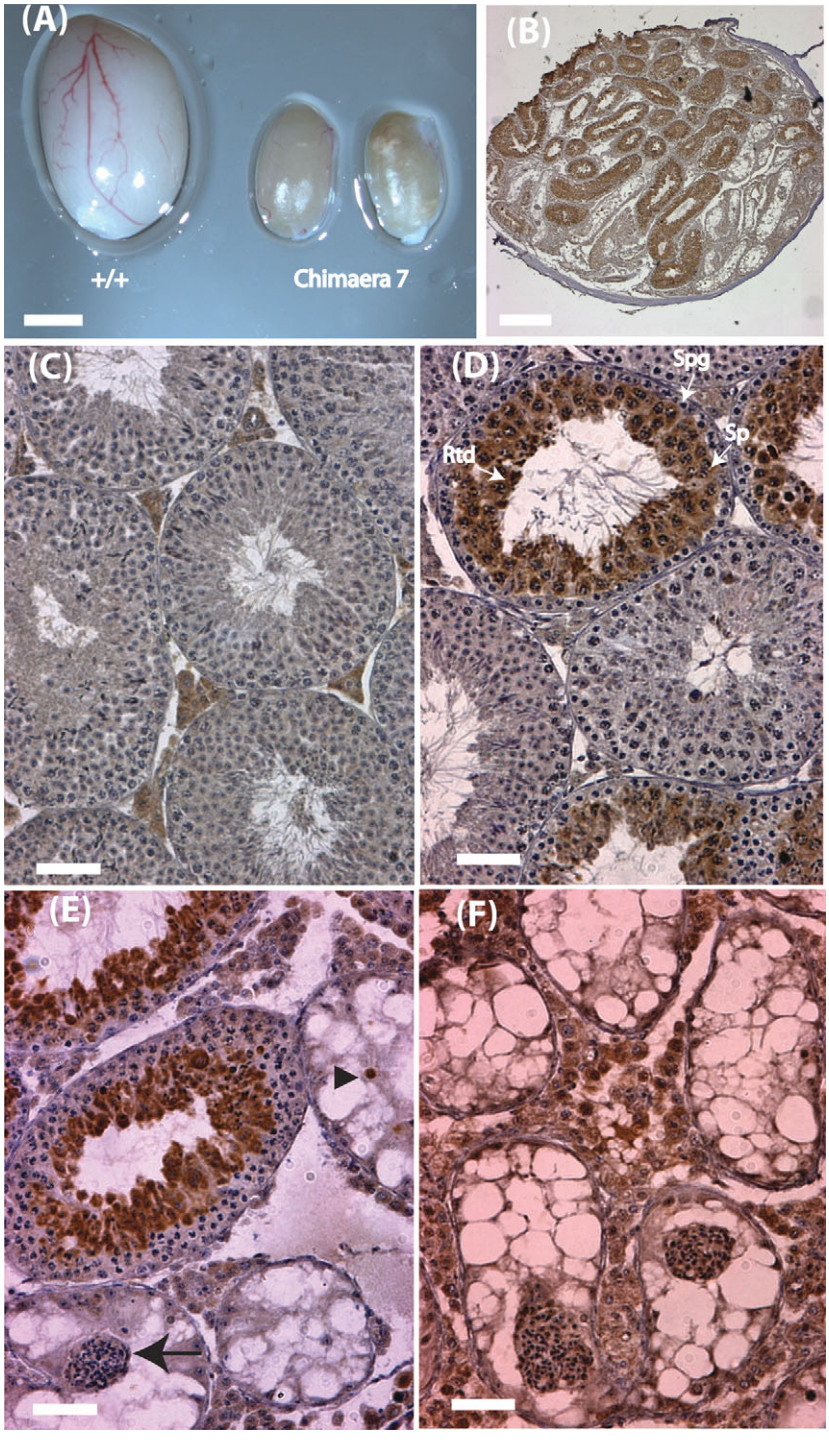

Figure 7. Testicular phenotype in chimaeric mice made from ES cell clone 2.1G5. (**A**) The two testes of chimaera 7 next to the testis of a C57Bl6 littermate (Scale bar = 2 mm). (**B**) A low resolution light micrograph of a section from chimaera C3 immunostained for LacZ (Scale bar = 20 μm). (**C**) High-resolution light micrograph of a testis section from a wild-type C57Bl6 littermate immunostained for LacZ. (**D**) High-resolution light micrograph of a testis section from chimaera C5 immunostained for LacZ. (**E**) High-resolution light micrograph of Chimaera C4 immunostained for LacZ. (**F**) High-resolution light micrograph of a testis section from Chimaera C7 immunostained for LacZ. Scale bars in (C)–(F) are equal to 50 μm.

by these chimaeras (Fig. 8A, lanes 2 and Fig. 8B, lane 4). We also tested genomic DNA extracted from the kidney to which the targeted ES129 cells had also contributed (Fig. 8A, lane 5 and Fig. 8B, lane 7).

Overall, these data suggested that despite a high contribution of targeted ES129 germ cells within the testes and epididymal sperm of chimaeras derived from 2.1G5, there was a failure to transmit the targeted allele, high levels of testicular

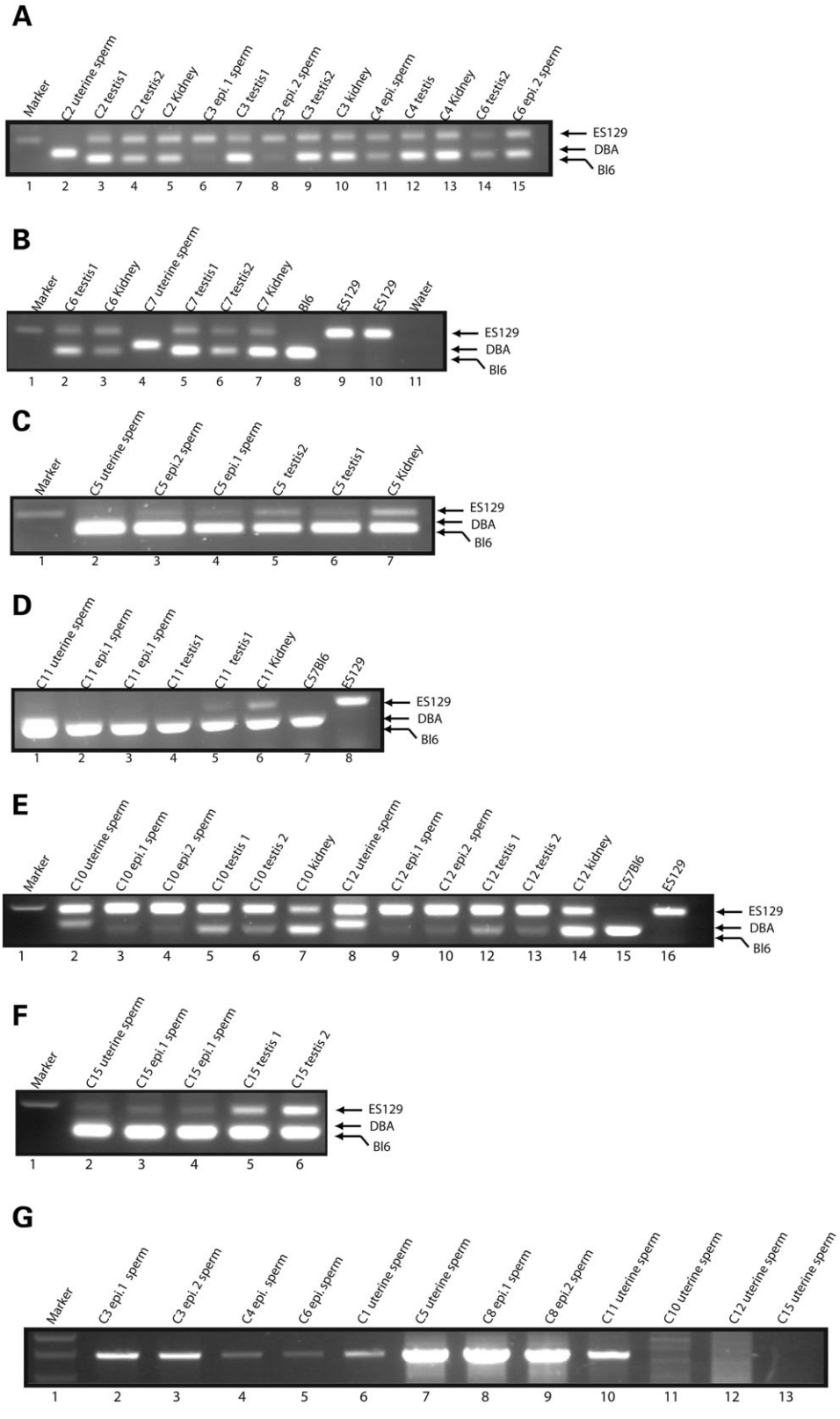

Figure 8. Genetic contribution of tissues and sperm from chimaeric mice made from ES cells containing the targeted allele of *Hnrnpgt*. (**A**–**F**) Genomic DNA was isolated from tissue, epididymal sperm or uterine sperm from plugged DBA females, amplified by genomic PCR and analysed by agarose gel electrophoresis to distinguish the cellular contribution of each genotype in the starting sample. (**G**) Genomic DNA was analysed using PCR primers to detect the targeted locus.

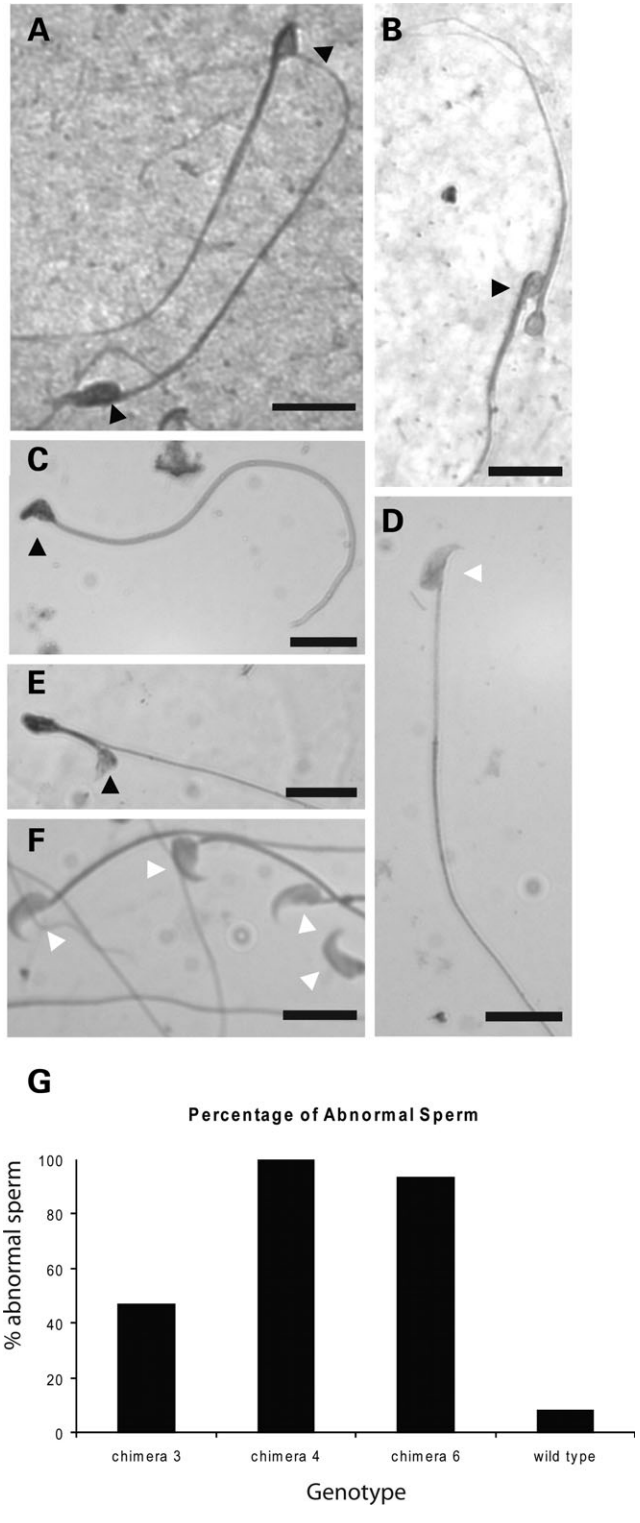

Figure 9. Sperm morphology of chimaeras and wild-type mice. Morphology of epididymal sperm from (**A** and **B**) chimaera C4; (**C**–**E**) chimaera C6 and (**F**) wild-type mouse prepared under identical conditions as detailed in Materials and Methods. Abnormal sperm heads are shown as a black arrow head, and normal sperm heads as a white arrow head. In each case, the scale bar represents 10 μm. (**G**) Bar chart showing the percentage abnormal sperm seen in each of three infertile chimaeras and the wild-type.

degeneration, low sperm counts and abnormal sperm morphology (summarized in Fig. 6). Full breeding data for these chimaeras are given in Supplementary Material, Table S4.

Chimaeric mice made from a heterogeneous clone containing wild-type and targeted ES cells only transmitted the wild-type allele

The above results suggested that germ cells which were haploinsufficient for the *Hnrnpgt* gene were unable to undergo functional spermatogenesis. To test this hypothesis, we next characterized the second E14.1 derived ES cell clone 3.1B11. Southern blot analysis of ES cell clone 3.1B11 revealed different signal intensities for wild-type and targeted alleles indicating a mixture of targeted and untargeted ES cells at a ratio of 1:1 (Fig. 5A and B). Importantly, both the targeted and wild-type ES cells within this clone 3.1B11 were passaged and processed identically during our experiments so the untargeted ES cells provide an internal control for the effectiveness of the targeted ES cells to functionally contribute to the germline. Karyotype analysis indicated 70% of clone 3.1B11 cells were euploid (Table 1).

Six fertile chimaeras with a high level of chimaerism judged by coat colour (four males and two females) were obtained from clone 3.1B11 (Supplementary Material, Table S4). Of these, C11 had a relatively low proportion of LacZ positive tubules detected by immunohistochemistry: less than 20% of the genomic DNA in the testis was from the 129 strain of mouse and some of the sperm contained the transgene therefore, this mouse was very similar to C1 and C8 derived from clone 2.1G5 (Fig. 6 and Fig. 8D and G). C11 produced 135 C57Bl6 pups, but also four agouti pups which did not contain the targeted mutation. In contrast, two of the other high percentage coat colour chimaeras derived from clone 3.1B11 (C10 and C12) had a much higher testicular ES129 contribution but no LacZ positive seminiferous tubules (Figs 6 and 8E). This suggested that the testes of C10 and C12 were mainly populated by the non-targeted ES129 cells within clone 3.1B11. We confirmed this by gene-specific PCR which showed that the targeted allele was not detected within uterine sperm from either chimaera (Fig. 8G). The testis of chimaera C10 also contained some apoptotic tubules which might have originally contained cells with the targeted allele. Both C10 and C12 fathered almost exclusively agouti pups (254/258) (Fig. 6 and Supplementary Material, Table S4) which were consistently negative for the targeted allele (data not shown). Even though C15 had low levels of ES129-derived sperm, this mouse still produced 41 agouti pups (Fig. 6). Unlike the samples from C5 and C11, none of the sperm contained the targeting construct (Fig. 8G) and the level of 129 genotype sperm did not decrease in the uterus relative to the epididymus (Fig. 8F). These experiments performed with a mixed population of wild-type ES cells grown in parallel with targeted ES cells indicate that wild-type but not targeted ES cells could result in the generation of functional sperm in chimaeric mice.

DISCUSSION

Our expression analysis indicates that *Hnrnpgt* provides the only source of an hnRNPG-like protein throughout meiosis

and post-meiotic germ cell development. This is a period of specialized cell division and intense differentiation which lasts up to 22 days in the mouse and considerably longer in humans. The expression of *Hnrnpgt* is thus likely to be fundamentally important for germ cell biology. Consistent with this the phylogenetic data in this paper indicate an ancient origin for the *HNRNPGT* gene prior to the divergence of the four main groups of placental mammals between 101 and 108 millions of years ago (15). To account for this evolutionary conservation, pairwise Ka/Ks analysis between human and mouse show that HNRNPGT genes are being maintained by positive selection. The conservation of *HNRNPGT* across evolutionary time is particularly compelling since our data also suggest that one of the other mouse *RBMX* genes (*Rbmxrt14*) is already starting to degenerate, despite its comparatively recent origin within the past million years in the rodent lineage. In addition to direct retrotransposition of *Rbmx*-derived transcripts generating autosomal retrogenes, our phylogenetic analyses indicate that *Rbmxrt14* is derived directly from *Rbmxrt8* rather than *Rbmx* itself. The evolution of a mouse retrogene derived from *Rbmxrt8* indicates that this retrotransposition must have occurred in the germline, and most likely from an *Rbmxrt8* transcript made within spermatogonia.

To test if the *Hnrnpgt* gene does play an important function in mouse spermatogenesis, we carried out gene targeting in ES cells and generated 22 chimaeras (19♂ and 3♀) from three independently targeted clones generated using two different starting lines of ES cells. Each of these chimaeras had a high level of chimaerism based on coat colour, normally a good prognostic indicator for germline transmission (19). The ES cells also had levels of euploidy much higher than that which would normally be consistent with germline transmission (18). Consistent with this, the lowest number of cells containing euploid chromosomes (70%) was actually observed in the cell line 3.1B11 which resulted in the highest number of agouti pups. Although we could detect 129 strain genomic contributions to the testis, germ cells and in some cases sperm, no agouti mice heterozygous for the targeted allele were born. In contrast, both E14.1-derived ES cell lines gave rise to wild-type agouti progeny, although at different ratios. These data suggest that the absence of one copy of the *Hnrnpgt* gene within targeted germ cells of chimaeric mice prevents transmission into the next generation. The phenotype of the chimaeras was variable, ranging from fertile (with low targeted ES129-contribution within the testis) to low sperm counts/abnormal sperm (with high targeted ES129-contribution within the testis) to azoospermic (with high targeted ES129-contribution within the testis). Chimaeric testes which contained a high percentage of heterozygosity for *Hnrnpgt* also had a high proportion of SCO tubules and were infertile. Some of the otherwise SCO tubules in these mice still contained a few residual germ cells which were LacZ-positive. Hence, the observed testicular degeneration in mice with high levels of chimaerism for *Hnrnpgt* targeted cells might have been progressive, and by extrapolation testes which were entirely devoid of germ cells might have initially contained germ cells heterozygous for the transgene. Consistent with this idea, one chimaera in our study (C4) had one small and one slightly larger testis. The progressive failure of spermatogenesis with age has been reported for a targeted mutation in another mouse gene (22) and is also implicated in some genetic cases of human male infertility (23). Although they did not transmit to the next generation, we could detect ES129-containing sperm in some of the 2.1G5-derived chimaeras. Noticeably, chimaera C5 had a much higher ES129 contribution relative to C57Bl6 than either chimaeras C11 and C15, but did not father any agouti pups. The experiments which showed that the amount of 129 cells in the uterine sperm decreased markedly in C5 relative to the epididymal sperm, whereas the wild-type 129 sperm which appeared in the uterus from C15 looked similar to the levels in the epididymus suggested a failure of the transgenic sperm to either survive in the uterus or leave the epididymus.

Overall, our data suggest that all the major stages of spermatogenesis can proceed within seminiferous tubules populated by germ cells containing a heterozygous deletion of *Hnrnpgt*, but functional sperm containing this deletion are not produced and there is a failure of seminiferous tubule survival in adult life. Hence depletion of *Hnrnpgt* is likely to be affecting the maintenance of germ cell differentiation in the adult chimaeras. Sperm produced in the infertile chimaeras were very abnormal in morphology, particularly in the sperm head. Sperm head abnormalities have also been reported for mice containing the Yd1 deletion which reduces *Rbmy* expression 50-fold (13). Decreases of *Rbmy* copy number might have a less severe phenotype than heterozygosity for *Hnrnpgt* possibly since reductions in *Rbmy* expression could be compensated for by active *Rbmx* and *Rbmxrt8* expression in spermatogonia (13,24–26). For the targeted allele in our experiments, most of the coding region of *Hnrnpgt* is replaced by *lacZ*. This is hence very likely to be a null allele resulting in reduced hnRNP G-T expression in targeted germ cells.

Two other retrogenes (*Jsd* and *tauCstF-64*) derived from X-linked genes have been shown to be essential for mouse spermatogenesis (27–29). In both these cases, heterozygous mice were fertile. However, some other chimaeric mice harbouring heterozygous disruptions of specific genes encoding important germ cell proteins are infertile. These include chimaeric mice containing germ cells heterozygous for the *Prm1 and Prm2* gene which encodes protamines responsible for packaging DNA in the sperm, in the *Klh10* gene which is also expressed in spermiogenesis, and in the *Pf20* and *Cyp17* genes (30–33). Biallelic expression might also be important for other RNA binding proteins expressed in germ cell development. Heterozygous deletions within the gene encoding the RNA binding protein *Dazl* also led to reduced testis size (34). The DAZL protein is thought to be primarily a translational regulator in the cytoplasm of meiotic and post-meiotic cells in adult life, but is nuclear in prenatal life (35).

Why might normal bi-allelic expression of hnRNPGT protein be essential for spermatogenesis? Unlike mitosis, transcription is very prolific in meiosis, which will generate an abundant source of pre-mRNA for splicing (36) and hnRNPG and hnRNPGT proteins are thought to function as a splicing factors (37,38). Splicing is thought to be controlled in part by the nuclear concentration of RNA binding proteins (39–41). Reductions in the nuclear concentration of hnRNP G-T protein over such a long developmental time window

Table 2. Sequences of primers used in this study

Name	Sequence (5′–3′)	Product Size (bp)	Mouse Strain
RbmxrtF	GGATCAAGGTCTCCATGCAA	140	
RbmxrtR	TCCTCACAAGAACACAAAAATGA		
RbmyF	AAGTTGTGTACCAAACAGCATTTC	312	
RbmyR	TTGACAGATTGTTTTTGACTATGC		
HnRNPGTF	GGACTGGCATCGGAAGTCTA	221	
HnRNPGTR	AACACGAGCTTGTTGAAACG		
Rbmxsplv1F	TCCCCAGTAAATGAGGCAAG	337	
Rbmxsplv1R	GGGGAAGGGAGGTTCTTGTA		
Rbmxsplv2F	TCTGCAATTTCGAGCTGATG	428	
Rbmxsplv2R	GCGTTCACATTACTGGCTGA		
TransgenF	TACCTAGGTCCCCACCATCA	2016	
TransgenR	GGCCTCTTCGCTATTACGC		
StrSpecF	GATCTTCTTTTATACACAAGTCATAGC	206	129
StrSpecR	GTGGTACAGAACTTAGGTGTTTAATTG	134	C57Bl6
		156	DBA

Unless otherwise specified Plantium *Taq* from Invitrogen was used for these PCRs.

might affect splice choices which are critically important for germ cell development. Consistent with dosage of RBMX proteins being important, the *RBMX* gene family contains two other active paralogues: *Rbmx* itself and *Rbmxrt8*. Our expression analysis showed that outside the testis, both *Rbmx* and *Rbmxrt8* (we assume from our above analysis that *Rbmxrt14* is not expressed) are both significantly upregulated in the thymus and spleen. Thymus and spleen are important sites for normal immune cell development which requires particularly high levels of alternative splicing (42) which might in turn require increased expression of RBMX proteins. The testis-expressed *RBMY* gene is also amplified on the mouse and human Y chromosomes, and so might provide increased levels of expression of this protein in spermatogonial cells. Hence, bi-allelic expression levels of *Hnrnpgt* might be required in the male mouse for normal gene expression pathways during and after meiosis when *Rbmx* and *Rbmxrt8* are not expressed. We postulate that by analogy both copies of *HNRNPGT* will be also required for normal human germ cell development, and that reductions in hnRNP G-T expression could similarly lead to reduced fertility in men.

MATERIALS AND METHODS

Strain-specific PCR

The strain-specific PCR primers StrSpecF and StrSpecR (Table 2) span a polymorphic locus and so yield different sized products depending on the strain of mouse. This PCR can distinguish between chromosomal DNA from the mouse strains 129 (ES cell line-derived) and C57Bl6 (blastocyst donor) which contributed to the chimaeras and DBA which is the strain used to isolate uterine sperm. The ratio of PCR products was quantitated (Genetools, SYNGENE) and used to determine the relative contribution of C57Bl/6, DBA and 129 within DNA samples. The uterine sperm samples were collected in DBA mice so that we would be able to differentiate between genomic DNA isolated from the sperm and contaminating genomic DNA from the female.

Targeted allele-specific PCR

The targeted allele was detected by a gene-specific PCR in which we utilize the primers TransgenF and TransgenR (Table 2). The primer TransgenF is located upstream of GT but outside the gene targeting vector and the primer TransgenR is located in lacZ. Therefore, a PCR product is only observed if the gene targeting vector is inserted in the correct place in the genome.

Purification of genomic DNA from sperm

Sperm were isolated from the uterus or epididymus either in PBS or Universal IVF fluid (Medicult) and purified according to manufacturer's directions using the Invisorb Spin Forensic kit (Invitek, Berlin).

Phylogenetic analysis

Putative hnRNPGT orthologues and RBMX sequences were identified using both BLAST, and through inspection of the Ensembl and UCSC databases, including multispecies Multiz alignments. Sequences were retrieved from Genbank (human *HNRNPGT*, accession number NM_014469; mouse *Hnrnpg*t, accession number AK005907), bull *HNRNPGT*, accession number BC114040; mouse *Rbmx* accession number NM_011252; human *RBMX*, accession number NM_002139; human *RBMXL1*, accession number NM_019610); the Sanger Centre (rat *Hnrnpgt*, ENSRNOG00000021946; mouse *Rbmxrt14*: ENSMUSG00000049235; Mouse *Rbmxrt8*: ENSMUSG00000037070); Macaque hnRNPGT NM_014469 Cow RBM AK096015; Rat RBMX NM_001079728; Rat RBMXRT8; Macaque RBMX NM_011252; and ENSEMBL: Tenrec hnRNPGT (ENSETEG00000005619) and Elephant

RBMX (ENSLAFG00000005568); and from UCSC (armadillo and elephant *HNRNPGT* were both assembled from UCSC vertebrate Multiz Alignments with human chromosome 11 between nucleotides 7066928 and 706888). Virtual translations of these sequences were aligned using Clustal X (43). Because the open reading frames of the Armadillo and Elephant hnRNPGT sequences were not intact (possibly due to the high throughput nature of the sequence data), these were excluded from the protein alignment, and were manually added to the multiple alignment at the nucleotide level. Trees constructed from the original protein alignment (excluding Armadillo and Elephant hnRNPGT sequences) gave the same two clade topology to that seen in Figure 1 (data not shown). Neighbour joining trees were constructed using the maximum composite likelihood method (44) with a Tamura-Nei model of evolution (45) using a shape parameter of 0.713 estimated from the data using FindModel (http://hcv.lanl.gov/content/hcv-db/findmodel/findmodel.html). All trees were constructed using MEGA4 software (46). Maximum Parsimony and Minimum Evolution trees were also constructed and had very similar topologies (not shown).

Divergence estimates

Mean Ks values and standard errors were estimated using the MEGA2.1 software package (47). We used the modified Nei-Gojobori method with Jukes-Cantor correction for multiple substitutions. We set the transition to transversion ratio (R) to 2.5 based on interspecific comparisons of mammalian genes (48). Preliminary alignments of predicted amino acid sequences were used to identify, and exclude from the analysis, regions of uncertain alignment and gaps resulting from deletion or insertion differences. Edited nucleotide sequences were then aligned using Clustal X and imported into MEGA for the analysis. We tested equality of mean Ks values by performing a Z test with type I error equal to 0.05.

Northern blots

RNA was purified from mouse tissues using Trizol reagent (Invitrogen, Carlsbad, CA, USA) according to manufacturer's directions. Fifteen micrograms of total RNA from each tissue was separated by electrophoresis on a 1% formaldehyde gel and blotted onto a Hybond N nylon membrane (Amersham). Because of the high level of sequence identity of *Rbmx* and *Rbmxrt8/14* within their open reading frames, we designed probes complementary to their 3′-UTRs. Radiolabelled probes were made from PCR products using either testis cDNA (for Rbmx splice variant 2) or cloned cDNAs (*Rbmx*splv1, *Rbmxrt8/14*, *Rbm* and *Hnrnpgt*) as a template using the primers shown in Table 2, or from a restriction fragment (*Gapdh)*. Probes were labelled by random priming with (α-^{32}P dNTPs) and were hybridized to membranes as previously described (2). After washing, the membranes were exposed to X-ray film overnight at -80 next to an intensifying screen. For quantitation, membranes were exposed on the Typhoon (GE healthcare) phosphorimager and band intensities measured and calculated using the Image Quant software. The amount of each transcript relative to the amount of the same transcript in the other tissues was measured to calculate a percentage of the total (if the same amount of transcript was expressed in each tissue then there would be 10% of the total in each of 10 tissues). To correct for loading, we normalized the percentage that we calculated relative to *Gapdh* (also a percentage) assuming that *Gapdh* is expressed equally in every tissue (shown numerically on the graph in Fig. 3).

Raising antisera specific to mouse hnRNPGT and hnRNPG

We generated and affinity purified a sheep antisera specific to the peptide GGRYDEYRGCSPDGYGG present within the conceptual ORF of mouse hnRNPGT and characterized this as reported previously (2). The detected protein corresponds to mouse hnRNP G-T since immuno-reactivity was pre-absorbed with the hnRNP G-T immunising peptide (Supplementary Fig. 2), and it exactly co-migrated with the testis-specific protein detected by the anti-human hnRNPG-T antiserum (2). A peptide antisera against hnRNPG protein was generated by immunizing rabbits with the peptide RDDGYSTKDC coupled to KLH. Antisera were affinity purified prior to usage.

Detection of proteins

Proteins from mouse tissues were homogenized in 2X sample buffer containing 4M urea (49), fractionated by SDS/PAGE and blotted onto a Millipore filter. Western filters were probed with sheep α-hnRNP G-T antiserum (1:500), rabbit α-hnRNPG antiserum (1:500) or rabbit α-Sam68 (Santa Cruz, dilution 1:1000); Rabbit α-ERK2 (Santa Cruz, dilution 1:1000); rabbit α-EIF4E (cell signalling, dilution 1:1000). Antisera were diluted in PBS-tween (0.1%) supplemented with 5% BSA.

Cell fractionation

Germ cell purification using elutriation, immunoprecipitations from extracts of purified germ cells and polysome fractionation were carried out as previously described (17).

Construction of gene targeting vector and generation of chimaeric mice

Accuprime High Fidelity *Taq* (Invitrogen) was used to generate the short arm and long arm of the targeting construct using TBV-2 ES cell genomic DNA as a template. The 5′-end containing the short arm was first cloned into plasmid psDKlacZpa so that the coding sequence of *Hnrnpgt* would be replaced by *lacZ*. Subsequently, a *Kpn*1-*Bam*HI fragment containing *lacZ* and 1.8 kb of sequence upstream of *Hnrnpgt* was cloned into a modified version of pKSloxPNTSKL (pKSloxPNTSKL+ polylinker). Finally, a *Xho*I-*Not*I fragment from pNeoflox-8 containing the neo cassette and a 5 kb *Pac*I-*Nhe*I fragment containing the long arm were inserted into the pKSloxPNTSKL+polylinker to yield the final gene targeting vector. The targeting vector was linearized with *Kpn*I and electroporated into the ES cells. ES cells were cultured on a layer of SNLP (clone 76/7-4) feeder cells (50). Culture conditions, electroporation, G418 and gangcyclovir selection and isolation, propagation and analysis of resistant

ES cell colonies were all as described (51). Resistant ES cell clones were screened by PCR with primers TransgenF and TransgenR (Table 2), and by Southern blot analysis (as shown in Fig. 5). Positive clones were microinjected into C57Bl/6 blastocysts. The resulting chimaeric mice were mated with C57Bl/6 females to screen for germ line transmission, and with DBA females for making uterine sperm samples. Karyotyping of ES cells was carried out by CHROMBIOS (Raubling, Germany).

Immunohistochemistry

Testes from the mice and humans were fixed in Bouins solution and embedded in paraffin wax. The sections were prepared according to standard procedures and the antigens were revealed by microwaving in 0.01M citrate buffer (pH6.0) (2). Either a 1:100 dilution of rabbit polyclonal antibody to β galactosidase (Abcam) or an equivalent concentration of rabbit IgG was incubated with the sections overnight for the mouse sections followed by a 1:400 dilution of biotinylated goat anti-rabbit (Dako) secondary antibody. The avidin-biotin-horseradish peroxidise system (ABC-HRP) and diaminobenzidine (Sigma) were utilized for antibody detection. Sections were counterstained in Harris haematoxylin and mounted in Histomount (National Diagnostics). The human testis sections were stained as previously described (11,52) using the antisera specific for hnRNPG and the DAB detection system. For immunofluroscence, the slides were not microwaved before incubation with antibody.

Sperm staining and morphology

Sperm were fixed and stained according to manufacturer's instructions using Spermac Stain (Stain Enterprises, RSA) and mounted with DPX. Two hundred sperm were counted in each sample and scored either as normal or abnormal based on morphology.

SUPPLEMENTARY MATERIAL

Supplementary Material is available at HMG Online.

ACKNOWLEDGEMENTS

We thank Professor Howard Cooke for helpful advice on the LacZ staining. We would also like to thank Kerstin Seidel for her help with the mice and useful discussions.

Conflict of Interest statement. None declared.

FUNDING

This work was funded by the Biotechnology and Biological Sciences Research Council (BBSRC Grant number G17920 to D.J.E.). C.D. was funded by the Special Trustees of the Royal Victoria Infirmary. The work in C.S.'s laboratory was supported by Telethon (grant GGP04118 to C.S.) and Lance Armstrong Foundation (to C.S.).

REFERENCES

1. Weighardt, F., Biamonti, G. and Riva, S. (1996) The roles of heterogeneous nuclear ribonucleoproteins (hnRNP) in RNA metabolism. *Bioessays*, **18**, 747–756.
2. Elliott, D.J., Venables, J.P., Newton, C.S., Lawson, D., Boyle, S., Eperon, I.C. and Cooke, H.J. (2000) An evolutionarily conserved germ cell-specific hnRNP is encoded by a retrotransposed gene. *Hum. Mol. Genet.*, **9**, 2117–2124.
3. Wang, P.J., Page, D.C. and McCarrey, J.R. (2005) Differential expression of sex-linked and autosomal germ-cell-specific genes during spermatogenesis in the mouse. *Hum. Mol. Genet.*, **14**, 2911–2918.
4. Turner, J.M., Mahadevaiah, S.K., Fernandez-Capetillo, O., Nussenzweig, A., Xu, X., Deng, C.X. and Burgoyne, P.S. (2005) Silencing of unsynapsed meiotic chromosomes in the mouse. *Nat. Genet.*, **37**, 41–47.
5. Turner, J.M., Mahadevaiah, S.K., Ellis, P.J., Mitchell, M.J. and Burgoyne, P.S. (2006) Pachytene asynapsis drives meiotic sex chromosome inactivation and leads to substantial postmeiotic repression in spermatids. *Dev. Cell*, **10**, 521–529.
6. Wang, P.J. (2004) X chromosomes, retrogenes and their role in male reproduction. *Trends Endocrinol. Metab.*, **15**, 79–83.
7. Lingenfelter, P.A., Delbridge, M.L., Thomas, S., Hoekstra, H.E., Mitchell, M.J., Graves, J.A. and Disteche, C.M. (2001) Expression and conservation of processed copies of the RBMX gene. *Mamm. Genome*, **12**, 538–545.
8. Mazeyrat, S., Saut, N., Mattei, M.G. and Mitchell, M.J. (1999) RBMY evolved on the Y chromosome from a ubiquitously transcribed X-Y identical gene. *Nat. Genet.*, **22**, 224–226.
9. Westerveld, G.H., Gianotten, J., Leschot, N.J., van der Veen, F., Repping, S. and Lombardi, M.P. (2004) Heterogeneous nuclear ribonucleoprotein G-T (HNRNP G-T) mutations in men with impaired spermatogenesis. *Mol. Hum. Reprod.*, **10**, 265–269.
10. Maymon, B.B., Paz, G., Elliott, D.J., Lifschitz-Mercer, B., Yogev, L., Kleiman, S.E., Botchan, A., Hauser, R., Schreiber, L. and Yavetz, H. (2002) Localization of the germ cell-specific protein, hnRNP G-T, in testicular biopsies of azoospermic men. *Acta Histochem.*, **104**, 255–261.
11. Elliott, D.J., Millar, M.R., Oghene, K., Ross, A., Kiesewetter, F., Pryor, J., McIntyre, M., Hargreave, T.B., Saunders, P.T., Vogt, P.H. *et al.* (1997) Expression of RBM in the nuclei of human germ cells is dependent on a critical region of the Y chromosome long arm. *Proc. Natl Acad. Sci. USA*, **94**, 3848–3853.
12. Elliott, D.J. (2000) RBMY genes and AZFb deletions. *J. Endocrinol. Invest.*, **23**, 652–658.
13. Mahadevaiah, S.K., Odorisio, T., Elliott, D.J., Rattigan, A., Szot, M., Laval, S.H., Washburn, L.L., McCarrey, J.R., Cattanach, B.M., Lovell-Badge, R. *et al.* (1998) Mouse homologues of the human AZF candidate gene RBM are expressed in spermatogonia and spermatids, and map to a Y chromosome deletion interval associated with a high incidence of sperm abnormalities. *Hum. Mol. Genet.*, **7**, 715–727.
14. Delbridge, M.L., Harry, J.L., Toder, R., O'Neill, R.J., Ma, K., Chandley, A.C. and Graves, J.A. (1997) A human candidate spermatogenesis gene, RBM1, is conserved and amplified on the marsupial Y chromosome. *Nat. Genet.*, **15**, 131–136.
15. Murphy, W.J., Eizirik, E., O'Brien, S.J., Madsen, O., Scally, M., Douady, C.J., Teeling, E., Ryder, O.A., Stanhope, M.J., de Jong, W.W. *et al.* (2001) Resolution of the early placental mammal radiation using Bayesian phylogenetics. *Science*, **294**, 2348–2351.
16. Waterston, R.H., Lindblad-Toh, K., Birney, E., Rogers, J., Abril, J.F., Agarwal, P., Agarwala, R., Ainscough, R., Alexandersson, M., An, P. *et al.* (2002) Initial sequencing and comparative analysis of the mouse genome. *Nature*, **420**, 520–562.
17. Paronetto, M.P., Zalfa, F., Botti, F., Geremia, R., Bagni, C. and Sette, C. (2006) The nuclear RNA-binding protein Sam68 translocates to the cytoplasm and associates with the polysomes in mouse spermatocytes. *Mol. Biol. Cell*, **17**, 14–24.
18. Longo, L., Bygrave, A., Grosveld, F.G. and Pandolfi, P.P. (1997) The chromosome make-up of mouse embryonic stem cells is predictive of somatic and germ cell chimaerism. *Transgenic Res.*, **6**, 321–328.
19. Fedorov, L.M., Haegel-Kronenberger, H. and Hirchenhain, J. (1997) A comparison of the germline potential of differently aged ES cell lines and their transfected descendants. *Transgenic Res.*, **6**, 223–231.
20. Kist, R., Greally, E. and Peters, H. (2007) Derivation of a mouse model for conditional inactivation of Pax9. *Genesis*, **45**, 460–464.

21. Kist, R., Watson, M., Wang, X., Cairns, P., Miles, C., Reid, D.J. and Peters, H. (2005) Reduction of Pax9 gene dosage in an allelic series of mouse mutants causes hypodontia and oligodontia. *Hum. Mol. Genet.*, **14**, 3605–3617.
22. Nayernia, K., Vauti, F., Meinhardt, A., Cadenas, C., Schweyer, S., Meyer, B.I., Schwandt, I., Chowdhury, K., Engel, W. and Arnold, H.H. (2003) Inactivation of a testis-specific Lis1 transcript in mice prevents spermatid differentiation and causes male infertility. *J. Biol. Chem.*, **278**, 48377–48385.
23. Reijo, R., Alagappan, R.K., Patrizio, P. and Page, D.C. (1996) Severe oligozoospermia resulting from deletions of azoospermia factor gene on Y chromosome. *Lancet*, **347**, 1290–1293.
24. Lee, J., Hong, J., Kim, E., Kim, K., Kim, S.W., Krishnamurthy, H., Chung, S.S., Wolgemuth, D.J. and Rhee, K. (2004) Developmental stage-specific expression of Rbm suggests its involvement in early phases of spermatogenesis. *Mol. Hum. Reprod.*, **10**, 259–264.
25. Turner, J.M., Mahadevaiah, S.K., Elliott, D.J., Garchon, H.J., Pehrson, J.R., Jaenisch, R. and Burgoyne, P.S. (2002) Meiotic sex chromosome inactivation in male mice with targeted disruptions of Xist. *J. Cell Sci.*, **115**, 4097–4105.
26. Saunders, P.T., Turner, J.M., Ruggiu, M., Taggart, M., Burgoyne, P.S., Elliott, D. and Cooke, H.J. (2003) Absence of mDazl produces a final block on germ cell development at meiosis. *Reproduction*, **126**, 589–597.
27. Bradley, J., Baltus, A., Skaletsky, H., Royce-Tolland, M., Dewar, K. and Page, D.C. (2004) An X-to-autosome retrogene is required for spermatogenesis in mice. *Nat. Genet.*, **36**, 872–876.
28. Rohozinski, J. and Bishop, C.E. (2004) The mouse juvenile spermatogonial depletion (jsd) phenotype is due to a mutation in the X-derived retrogene, mUtp14b. *Proc. Natl Acad. Sci. USA*, **101**, 11695–11700.
29. Dass, B., Tardif, S., Park, J.Y., Tian, B., Weitlauf, H.M., Hess, R.A., Carnes, K., Griswold, M.D., Small, C.L. and Macdonald, C.C. (2007) Loss of polyadenylation protein tauCstF-64 causes spermatogenic defects and male infertility. *Proc. Natl Acad. Sci. USA*, **104**, 20374–20379.
30. Cho, C., Willis, W.D., Goulding, E.H., Jung-Ha, H., Choi, Y.C., Hecht, N.B. and Eddy, E.M. (2001) Haploinsufficiency of protamine-1 or -2 causes infertility in mice. *Nat. Genet.*, **28**, 82–86.
31. Yan, W., Ma, L., Burns, K.H. and Matzuk, M.M. (2004) Haploinsufficiency of kelch-like protein homolog 10 causes infertility in male mice. *Proc. Natl Acad. Sci. USA*, **101**, 7793–7798.
32. Zhang, Z., Kostetskii, I., Moss, S.B., Jones, B.H., Ho, C., Wang, H., Kishida, T., Gerton, G.L., Radice, G.L. and Strauss, J.F., 3rd (2004) Haploinsufficiency for the murine orthologue of Chlamydomonas PF20 disrupts spermatogenesis. *Proc. Natl Acad. Sci. USA*, **101**, 12946–12951.
33. Liu, Y., Yao, Z.X., Bendavid, C., Borgmeyer, C., Han, Z., Cavalli, L.R., Chan, W.Y., Folmer, J., Zirkin, B.R., Haddad, B.R. *et al.* (2005) Haploinsufficiency of cytochrome P450 17alpha-hydroxylase/17,20 lyase (CYP17) causes infertility in male mice. *Mol. Endocrinol.*, **19**, 2380–2389.
34. Ruggiu, M., Speed, R., Taggart, M., McKay, S.J., Kilanowski, F., Saunders, P., Dorin, J. and Cooke, H.J. (1997) The mouse Dazla gene encodes a cytoplasmic protein essential for gametogenesis. *Nature*, **389**, 73–77.
35. Reijo, R.A., Dorfman, D.M., Slee, R., Renshaw, A.A., Loughlin, K.R., Cooke, H. and Page, D.C. (2000) DAZ family proteins exist throughout male germ cell development and transit from nucleus to cytoplasm at meiosis in humans and mice. *Biol. Reprod.*, **63**, 1490–1496.
36. Monesi, V. (1964) Ribonucleic acid synthesis during mitosis and meiosis in the mouse testis. *J. Cell Biol.*, **22**, 521–532.
37. Elliott, D.J. (2004) The role of potential splicing factors including RBMY, RBMX, hnRNPG-T and STAR proteins in spermatogenesis. *Int. J. Androl.*, **27**, 328–334.
38. Nasim, M.T., Chernova, T.K., Chowdhury, H.M., Yue, B.G. and Eperon, I.C. (2003) HnRNP G and Tra2beta: opposite effects on splicing matched by antagonism in RNA binding. *Hum. Mol. Genet.*, **12**, 1337–1348.
39. Park, J.W., Parisky, K., Celotto, A.M., Reenan, R.A. and Graveley, B.R. (2004) Identification of alternative splicing regulators by RNA interference in Drosophila. *Proc. Natl Acad. Sci. USA*, **101**, 15974–15979.
40. Matlin, A.J., Clark, F. and Smith, C.W. (2005) Understanding alternative splicing: towards a cellular code. *Nat. Rev. Mol. Cell Biol.*, **6**, 386–398.
41. Fu, X.D. (2004) Towards a splicing code. *Cell*, **119**, 736–738.
42. Lynch, K.W. (2004) Consequences of regulated pre-mRNA splicing in the immune system. *Nat. Rev. Immunol.*, **4**, 931–940.
43. Thompson, J.D., Gibson, T.J., Plewniak, F., Jeanmougin, F. and Higgins, D.G. (1997) The CLUSTAL_X windows interface: flexible strategies for multiple sequence alignment aided by quality analysis tools. *Nucleic Acids Res.*, **25**, 4876–4882.
44. Kumar, S., Tamura, K. and Nei, M. (1994) MEGA: Molecular Evolutionary Genetics Analysis software for microcomputers. *Comput. Appl. Biosci.*, **10**, 189–191.
45. Tamura, K. and Nei, M. (1993) Estimation of the number of nucleotide substitutions in the control region of mitochondrial DNA in humans and chimpanzees. *Mol. Biol. Evol.*, **10**, 512–526.
46. Tamura, K., Dudley, J., Nei, M. and Kumar, S. (2007) MEGA4: Molecular Evolutionary Genetics Analysis (MEGA) software version 4.0. *Mol. Biol. Evol.*, **24**, 1596–1599.
47. Kumar, S., Tamura, K., Jakobsen, I.B. and Nei, M. (2001) MEGA2: molecular evolutionary genetics analysis software. *Bioinformatics*, **17**, 1244–1245.
48. Rosenberg, M.S., Subramanian, S. and Kumar, S. (2003) Patterns of transitional mutation biases within and among mammalian genomes. *Mol. Biol. Evol.*, **20**, 988–993.
49. Venables, J.P., Dalgliesh, C., Paronetto, M.P., Skitt, L., Thornton, J.K., Saunders, P.T., Sette, C., Jones, K.T. and Elliott, D.J. (2004) SIAH1 targets the alternative splicing factor T-STAR for degradation by the proteasome. *Hum. Mol. Genet*, **13**, 1525–1534.
50. McMahon, A.P. and Bradley, A. (1990) The Wnt-1 (int-1) proto-oncogene is required for development of a large region of the mouse brain. *Cell*, **62**, 1073–1085.
51. Matise, M.P., Auerbach, W. and Joyner, A.L. (2000) Production of targeted embryonic stem cell clones. Joyner, A.L. (eds), *Gene Targeting: A Practical Approach*, 2nd edn. Oxford University Press, Oxford, UK, pp. 101–132.
52. Elliott, D.J., Oghene, K., Makarov, G., Makarova, O., Hargreave, T.B., Chandley, A.C., Eperon, I.C. and Cooke, H.J. (1998) Dynamic changes in the subnuclear organisation of pre-mRNA splicing proteins and RBM during human germ cell development. *J. Cell Sci.*, **111**, 1255–1265.